Preprints of the 21st IFAC World Congress (Virtual)
Berlin, Germany, July 12-17, 2020

Kinematic Control of Serial Manipulators Using Clifford Algebra ⋆

A. Shahidi * **M. Hüsing** * **B. Corves** *

* *Institute of Mechanism Theory, Machine Dynamics and Robotics, RWTH Aachen University, D-52072 Aachen, Germany (e-mail: {shahidi, huesing, corves}@igmr.rwth-aachen.de)*

Abstract: We exploit the potentials of Clifford algebra to present a singularity free, compact, and computationally efficient scheme for kinematic control of serial manipulators. We introduce and implement the new *special proportional-derivative* control scheme. The introduced control scheme facilitates a fast motion control for the manipulators and enables them to react to the changes in their set points quickly. Such conditions are common in the context of dynamic working environments and collaborative manipulation scenarios. We describe the kinematics of the manipulators with unit dual quaternions using screw theory. The Lie-group properties of quaternions and dual quaternions are presented and discussed. By means of Lyapunov theory, it will be shown that the controller is globally exponentially stable.

Keywords: Motion Control, Robot Manipulators, Clifford Algebra, Dual Quaternions

1. INTRODUCTION

This paper presents the kinematic control of serial manipulators using Clifford algebra of unit dual quaternions. To describe a kinematic chain, one needs the transformation tools. Unit dual quaternions have the potential to encapsulate the translation and rotation in a simple and compact form. This fact enables us to embed the position of the joints beside their state.

There has been a number of comparative studies over different descriptions of transformation, which report the unit dual quaternions as the most compact and efficient one (see for instance Funda et al. (1990) and Wang and Zhu (2014)). For an overview on different representation attitudes we refer to Diebel (2006). A geometrical overview on the dual quaternions besides the attitude control of a quad-rotor have been presented by Wang et al. (2012).

In a recent work Özgür and Mezouar (2016) presented a model for forward position kinematics of serial robot using dual quaternions and compared the mathematical cost of different transformation methods. Olsson et al. (2003) used unit dual quaternions to model the camera and end-effector in a hand-eye calibration to track the position of objects. Stolt et al. (2012) utilized the orientation representation of quaternions to avoid singularities in assembly tasks. Attitude control of objects using dual quaternions is discussed by Han et al. (2008) and Dapeng et al. (2007). Clifford algebra for synthesis of serial spatial chains also has been discussed by Perez-Gracia and McCarthy (2006).

We present a self-sufficient and comprehensive paper in kinematic control using Clifford algebra. Mathematical background of quaternions and dual quaternions will be presented and their properties as group will be introduced (for more in these topics we refer to Wang et al. (2012); Dapeng et al. (2007)). In this paper we adopt this mathematical operation in the context of robotics. We also present a new *special proportional-derivative* control scheme for kinematic control of the manipulators. The stability of the controller will be discussed via Lyapunov method using the norm function of logarithmic mapping of the pose-error as Lyapunov function candidate.

⋆ The Authors would like to thank for the kind support of German Research Foundation DFG (Deutsche Forschungsgemeinschaft) under Germany's Excellence Strategy – EXC-2023 Internet of Production – 390621612.

NOMENCLATURE

$\hat{Q}$ Quaternion
$\hat{Q} = [\hat{q}, \hat{\boldsymbol{q}}] \in \mathbb{H} \simeq \mathbb{R}^4$

$\hat{\boldsymbol{q}}$ Pure Quaternion
$\hat{\boldsymbol{q}} = (\hat{\boldsymbol{q}}_x\, i + \hat{\boldsymbol{q}}_y\, j + \hat{\boldsymbol{q}}_z\, k) \in \mathbb{H}^{\mathcal{V}} \simeq \mathbb{R}^3$
i, j & k; Quaternionic units,
$i^2 = j^2 = k^2 = i\,j\,k = -1$

$\bar{d}$ Dual Number
$\bar{d} = \langle d_p, d_d \rangle = d_p + \epsilon\, d_d$, $\bar{d} \in \mathbb{D}$
ϵ; Nilpotent Clifford unit, $\epsilon^2 = 0$

$\breve{D}$ Dual Quaternion
$\breve{D} = \left\langle \breve{d}, \breve{\boldsymbol{d}} \right\rangle \in \mathbb{H}^2$

$\breve{D}$ Dual Quaternion
$\breve{D} = [\breve{d}, \breve{\boldsymbol{d}}] \in \mathbb{D}^4$

$\breve{D}, \breve{D} \in \mathbb{DH}$ $(\mathbb{DH} \equiv \mathbb{D} \times \mathbb{H})$

$\breve{\boldsymbol{d}}$ Dual Vector
$\breve{\boldsymbol{d}} = \left(\bar{d}_1\,, \bar{d}_2\, \ldots\,, \bar{d}_n\right) \in \mathbb{D}^n \simeq \mathbb{R}^{2n}$
$\breve{\boldsymbol{d}} = \langle \breve{\boldsymbol{d}}_p\,, \breve{\boldsymbol{d}}_d \rangle$

Note that in this paper, we distinguish between different representation structures of dual quaternions, that is, a dual whose primal and dual parts are quaternions ($\check{D}$) and a quaternion with dual members ($\check{D}$). The reason behind this separation is the simplicity of mathematical operation in different forms (*cf. Appendix C*).

2. MATHEMATICAL BACKGROUND

The Clifford algebra is well known for its potential for generalization in different fields, *e.g.* real and complex numbers, quaternions, and other hyper-complex numbers. Clifford algebra over a set $\mathbb{O}$ is described by $C\ell_{x,y,z}(\mathbb{O})$, with x, y and z denoting the number of generators e that square to 1, -1 and 0 respectively and $\mathbb{O}$ indicating the set on which the algebra is being defined. The generators of Clifford algebra anti-commute, that is

$$e_n e_m + e_m e_n = 0.$$

Obviously $C\ell_{0,0,0}(\mathbb{R})$ refers to geometric algebra and is isomorphic to $\mathbb{R}$. We refer to Hestenes and Sobczyk (2012) for more on Clifford algebra. In the following the Clifford algebra for quaternions and dual quaternions are discussed, which we use to describe the kinematic structure of the manipulators.

2.1 Quaternions

Quaternions, introduced by Hamilton (1848), are $4-$tuples over the set of real numbers associated to $C\ell_{0,2,0}(\mathbb{R})$ with the generators e_1 and e_2,

$$\begin{aligned} e_1^2 &= -1, & e_1 &\cong i, \\ e_2^2 &= -1, & e_2 &\cong j, \\ e_1\, e_2\, e_1\, e_2 &= -e_1\, e_1\, e_2\, e_2 = -e_1^2\, e_2^2 \;\therefore \\ (e_1\, e_2)^2 &= -1, & e_1\, e_2 &\cong k. \end{aligned}$$

Some mathematical properties of the quaternions are presented in *Appendix A*.

Definition 2.1.1. Quaternions with $\left|\hat{Q}\right| = 1$ are known as unit quaternions, forming the set $\mathbb{H}_{\mathcal{U}} \subset \mathbb{H}$.

Definition 2.1.2. The unit quaternions of the form

$$\hat{R} = \left[\cos\left(\frac{\theta}{2}\right) \,,\, \sin\left(\frac{\theta}{2}\right)\hat{\boldsymbol{l}}\right],\;\; \theta \in [-\pi\,,\,\pi), \tag{1}$$

are known as *angle representation*, $\hat{R} \in \mathbb{H}_{\mathcal{U}}$, where $\hat{\boldsymbol{l}}$ (unit pure quaternion) represents the rotation axis (*cf. Section 3*)

Lemma 2.1. $\mathbb{H}_{\mathcal{U}}$ is a Lie-group.

Proof: $\mathbb{H}_{\mathcal{U}}$ is a group under $\circ$.

Identity element: $\hat{I} = [1, \hat{\mathbf{0}}]$.
Inverse element: the conjugate of a unit quaternion is its inverse.
Closure: for $\hat{Q}_1$ and $\hat{Q}_2 \in \mathbb{H}_{\mathcal{U}}$, $\hat{Q}_1 \circ \hat{Q}_1^* = \hat{Q}_2 \circ \hat{Q}_2^* = \hat{Q}_1 \circ \hat{Q}_2 \circ \hat{Q}_2^* \circ \hat{Q}_1^* = (\hat{Q}_1 \circ \hat{Q}_2) \circ (\hat{Q}_1 \circ \hat{Q}_2)^* = \hat{I}$, hence $(\hat{Q}_1 \circ \hat{Q}_2) \in \mathbb{H}_{\mathcal{U}}$.
Associate: for $\hat{Q}_1$, $\hat{Q}_2$, and $\hat{Q}_3 \in \mathbb{H}_{\mathcal{U}}$, after algebraic expansion and simplification, it is straightforward to investigate that $(\hat{Q}_1 \circ \hat{Q}_2) \circ \hat{Q}_3 = \hat{Q}_1 \circ (\hat{Q}_2 \circ \hat{Q}_3)$.

It can be shown that $\mathbb{H}_{\mathcal{U}}$ is diffeomorphic to manifold $\mathbb{S}^3$ (*cf.* Marsden and Ratiu (2013)), hence $\mathbb{H}_{\mathcal{U}}$ is a three dimensional manifold, thus a Lie-group. □

Definition 2.1.3. The exponential form of *angle representation* $\hat{R}$ reads as

$$\hat{R} = \exp\left(\left[0, \frac{\theta}{2}\hat{\boldsymbol{l}}\right]\right) \tag{2}$$

(note the analogy to the Euler formula in complex set $\mathcal{C}$).

Definition 2.1.4. Following the *Definition 2.1.3*, given an *angle representation* $\hat{R}$, one can define its logarithmic mapping as

$$\ln^{\mathbb{H}}(\hat{R}) = \left[0, \cos^{-1}(\hat{r})\, \frac{\hat{\boldsymbol{r}}}{|\hat{\boldsymbol{r}}|}\right], \tag{3}$$

with $|\bullet|$ denoting the euclidean norm. Obviously $\ln^{\mathbb{H}} : \mathbb{H}_{\mathcal{U}} \to \mathbb{H}^{\mathcal{V}}$.

Lemma 2.2. logarithmic mapping of unit quaternions is the Lie-algebra of $\mathbb{H}_{\mathcal{U}}$.

Proof: Picking $\hat{\boldsymbol{v}}_1$, $\hat{\boldsymbol{v}}_2$, and $\hat{\boldsymbol{v}}_3 \in \mathbb{H}^{\mathcal{V}}$, arbitrary constants λ_1 and $\lambda_2 \in \mathbb{R}$ and defining Lie-bracket as:

$$[\hat{\boldsymbol{v}}_n, \hat{\boldsymbol{v}}_m] = \hat{\boldsymbol{v}}_n \times \hat{\boldsymbol{v}}_m,\;\; n, m \in \{1, 2, 3\},$$

we test the following conditions:

Bilinearity:
$$[\lambda_1\, \hat{\boldsymbol{v}}_1 + \lambda_2\, \hat{\boldsymbol{v}}_2,\, \hat{\boldsymbol{v}}_3] = \lambda_1\, [\hat{\boldsymbol{v}}_1,\, \hat{\boldsymbol{v}}_3] + \lambda_2\, [\hat{\boldsymbol{v}}_2,\, \hat{\boldsymbol{v}}_3]\,.$$
Antisymmetric: $[\hat{\boldsymbol{v}}_1,\, \hat{\boldsymbol{v}}_2] = -[\hat{\boldsymbol{v}}_2,\, \hat{\boldsymbol{v}}_1]\,.$
Jacobi identity:
$$[[\hat{\boldsymbol{v}}_1,\, \hat{\boldsymbol{v}}_2]\,,\, \hat{\boldsymbol{v}}_3] + [[\hat{\boldsymbol{v}}_2,\, \hat{\boldsymbol{v}}_3]\,,\, \hat{\boldsymbol{v}}_1] + [[\hat{\boldsymbol{v}}_3,\, \hat{\boldsymbol{v}}_1]\,,\, \hat{\boldsymbol{v}}_2] = \hat{\mathbf{0}}.$$

The tangent of $\mathbb{H}_{\mathcal{U}}$ at unity $\hat{I}$ is defined as

$$\dot{\hat{Q}} = \frac{1}{2}\,\hat{\boldsymbol{\omega}} \circ \hat{Q}|_{\hat{Q}=\hat{I}} = \frac{1}{2}\,\hat{\boldsymbol{\omega}} \in \mathbb{H}^{\mathcal{V}} \simeq \mathbb{R}^3, \tag{4}$$

where $\hat{\boldsymbol{\omega}} = [0, \dot{\theta}\hat{\boldsymbol{l}}]$ denotes the angular velocity. Hence logarithmic mapping is the Lie-algebra of $\mathbb{H}_{\mathcal{U}}$. □

Definition 2.1.5. The adjoint mapping of quaternions $Ad_{\hat{Q}}\hat{X}$ is defined as

$$Ad_{\hat{Q}}\hat{X} = \hat{Q} \circ \hat{X} \circ \hat{Q}^*. \tag{5}$$

2.2 Dual Quaternions

Dual quaternions, introduced by Clifford (1873), are $8-$tuples over the set of real numbers associated to $C\ell_{0,2,1}(\mathbb{R})$ with generators e_1, e_2 and e_3,

$$\begin{aligned} e_1^2 &= -1, & e_1 &\cong i, \\ e_2^2 &= -1, & e_2 &\cong j, \\ (e_1\, e_2)^2 &= -1, & e_1\, e_2 &\cong k, \\ e_3^2 &= 0, & e_3 &\cong \epsilon. \end{aligned}$$

Some mathematical properties of the dual quaternions are presented in *Appendix B*.

Definition 2.2.1. Dual quaternions with unit norm are known as unit dual quaternions, forming the set $\mathbb{DH}_{\mathcal{U}} \subset \mathbb{DH}$.

Definition 2.2.2. The *angle representation* of unit dual quaternions, denoted by $\check{R} \in \mathbb{DH}_{\mathcal{U}}$, is defined as

$$\check{R} = \left[\cos\left(\frac{\bar{\theta}}{2}\right), \sin\left(\frac{\bar{\theta}}{2}\right)\,\ell\right],$$

with $\bar{\theta}$ known as dual angle of screw and ℓ represents the Plücker coordinate of the screw axis line (see *Section 3*).

Lemma 2.3. $\mathbb{DH}_{\mathcal{U}}$ is a Lie-group.

Proof: $\mathbb{DH}_{\mathcal{U}}$ is a group under $\diamond$.

Identity element: $\breve{I} = \left\langle \hat{I}, \hat{0} \right\rangle$.

Inverse element: the conjugate of a unit dual quaternion is its inverse.

Closure: for $\breve{D}_1$ and $\breve{D}_2 \in \mathbb{DH}_{\mathcal{U}}$, $\breve{D}_1 \diamond \breve{D}_1^* = \breve{D}_2 \diamond \breve{D}_2^* = \breve{D}_1 \diamond \breve{D}_2 \diamond \breve{D}_2^* \diamond \breve{D}_1^* = (\breve{D}_1 \diamond \breve{D}_2) \diamond (\breve{D}_1 \diamond \breve{D}_2)^* = \breve{I}$, hence $(\breve{D}_1 \diamond \breve{D}_2) \in \mathbb{DH}_{\mathcal{U}}$.

Associate: for $\breve{D}_1$, $\breve{D}_2$ and $\breve{D}_3 \in \mathbb{H}_{\mathcal{U}}$, after algebraic expansion and simplification, it is straightforward to investigate that $(\breve{D}_1 \diamond \breve{D}_2) \diamond \breve{D}_3 = \breve{D}_1 \diamond (\breve{D}_2 \diamond \breve{D}_3)$.

According to *Lemma 2.1*, $\mathbb{H}_{\mathcal{U}}$ is a three dimensional manifold. Expanding $\breve{D} \diamond \breve{D}^* = \breve{I}$ it can be shown that $\breve{d} \in \mathbb{H}_{\mathcal{U}}$ and $\boldsymbol{\breve{d}} \in \mathbb{H}^{\mathcal{V}}$. Hence $\mathbb{DH}_{\mathcal{U}}$ is a six dimensional manifold, thus a Lie-group. □

Lemma 2.4. The exponential form of *angle representation* of $\breve{R} \in \mathbb{DH}_{\mathcal{U}}$ in *Definition 2.2.2* reads as

$$\breve{R} = \exp\left(\left[\bar{0}, \frac{\bar{\theta}}{2} \diamond \ell\right]\right). \tag{6}$$

Proof: See *Appendix C.* □

Definition 2.2.3. Following the *Lemma 2.4*, given an *angle representation* $\breve{R}$, one can define its logarithmic mapping as

$$\ln^{\mathbb{DH}}(\breve{R}) = \left[\bar{0}, \frac{\bar{\theta}}{2} \diamond \ell\right] = \left\langle \hat{\boldsymbol{l}}'_p, \hat{\boldsymbol{l}}'_d \right\rangle. \tag{7}$$

Obviously $\ln^{\mathbb{DH}} : \mathbb{DH}_{\mathcal{U}} \to \mathbb{DH}^{\mathcal{V}}$, *i.e.* $\hat{\boldsymbol{l}}'_p \,\&\, \hat{\boldsymbol{l}}'_d \in \mathbb{H}^{\mathcal{V}}$.

Lemma 2.5. logarithmic mapping of unit dual quaternions is the Lie-algebra of $\mathbb{DH}_{\mathcal{U}}$.

Proof: Picking $\breve{\boldsymbol{v}}_1$, $\breve{\boldsymbol{v}}_2$ and $\breve{\boldsymbol{v}}_3 \in \mathbb{DH}^{\mathcal{V}}$, arbitrary constants λ_1 and $\lambda_2 \in \mathbb{R}$ and defining Lie-bracket as:

$$[\breve{\boldsymbol{v}}_n, \breve{\boldsymbol{v}}_m] = \breve{\boldsymbol{v}}_n \diamond \breve{\boldsymbol{v}}_m - \breve{\boldsymbol{v}}_m \diamond \breve{\boldsymbol{v}}_n, \;\; n, m \in \{1, 2, 3\},$$

we test the following conditions.

Bilinearity:

$$[\lambda_1 \breve{\boldsymbol{v}}_1 + \lambda_2 \breve{\boldsymbol{v}}_2, \breve{\boldsymbol{v}}_3] = \lambda_1 [\breve{\boldsymbol{v}}_1, \breve{\boldsymbol{v}}_3] + \lambda_2 [\breve{\boldsymbol{v}}_2, \breve{\boldsymbol{v}}_3].$$

Antisymmetric: $[\breve{\boldsymbol{v}}_1, \breve{\boldsymbol{v}}_2] = -[\breve{\boldsymbol{v}}_2, \breve{\boldsymbol{v}}_1]$. This result can be followed by expanding the dual multiplication of $\breve{\boldsymbol{v}}_1 = \langle \hat{\boldsymbol{v}}_{1,p}, \hat{\boldsymbol{v}}_{1,d} \rangle$ and $\breve{\boldsymbol{v}}_2 = \langle \hat{\boldsymbol{v}}_{2,p}, \hat{\boldsymbol{v}}_{2,d} \rangle$ and applying the quaternions multiplication $\circ$ (*cf. Appendix A*).

Jacobi identity: Algebraic expansion and simplification, using *Appendix B*, it can be seen

$$[[\breve{\boldsymbol{v}}_1, \breve{\boldsymbol{v}}_2], \breve{\boldsymbol{v}}_3] + [[\breve{\boldsymbol{v}}_2, \breve{\boldsymbol{v}}_3], \breve{\boldsymbol{v}}_1] + [[\breve{\boldsymbol{v}}_3, \breve{\boldsymbol{v}}_1], \breve{\boldsymbol{v}}_2] = \breve{\boldsymbol{0}}.$$

The tangent of $\mathbb{DH}_{\mathcal{U}}$ at unity $\breve{I}$ is defined as

$$\dot{\breve{D}} = \frac{1}{2} \breve{\Xi} \diamond \breve{D}|_{\breve{D}=\breve{I}} = \frac{1}{2} \breve{\Xi} \in \mathbb{DH}^{\mathcal{V}} \simeq \mathbb{R}^6.$$

Hence logarithmic mapping is the Lie-algebra of $\mathbb{DH}_{\mathcal{U}}$. (Note: $\breve{\Xi} = \left\langle \hat{\boldsymbol{\omega}}, \dot{\hat{\boldsymbol{d}}} + \hat{\boldsymbol{p}} \times \hat{\boldsymbol{\omega}} \right\rangle$ denotes the twist – *cf. Section 3.*) □

Definition 2.2.4. The adjoint mapping of dual quaternions $Ad^k_{\breve{D}} \breve{X}$ is defined as

$$Ad^k_{\breve{D}} \breve{X} = \breve{D} \diamond \breve{X} \diamond \breve{D}^{*_k}, \; k \in \{0, 1, 2\}. \tag{8}$$

If $k = 1$, we drop the superscript for simplicity of notation (see *Appendix B* for definition of k).

Definition 2.2.5. The norm of the logarithm mapping of unit dual quaternions in *Definition 2.2.3* can be defined as (*cf.* Wang et al. (2012))

$$\left\| \ln^{\mathbb{DH}}(\breve{R}) \right\| = \alpha \left| \hat{\boldsymbol{l}}'_p \right| + \beta \left| \hat{\boldsymbol{l}}'_d \right|, \tag{9}$$

with α and $\beta \in \mathbb{R}_+$.

Definition 2.2.6. Plücker coordinate of a line: A line ℓ in the space can be determined by its direction $\hat{\boldsymbol{l}}$ and an arbitrary point $\hat{\boldsymbol{p}}$ on it. The lines can be presented as a dual quaternions

$$\ell = \left\langle \hat{\boldsymbol{l}}, \hat{\boldsymbol{p}} \times \hat{\boldsymbol{l}} \right\rangle, \tag{10}$$

where $\hat{\boldsymbol{p}} \times \hat{\boldsymbol{l}}$ is known as the moment of the line $\hat{\boldsymbol{m}}$.

3. KINEMATIC MODELING

3.1 Rigid Body Transformation

It is well known that the rotation by $\theta \in [-\pi, \pi)$ about the unit axis of a line direction $\hat{\boldsymbol{l}}$ can be formulated by the *angle representation* $\hat{R} \in \mathcal{H}_{\mathcal{U}}$. This rotation is defined via adjoint mapping of quaternions, *Definition 2.1.5*, that is, given a point $\hat{\boldsymbol{p}}_1 \in \mathcal{R}^3$, its rotation is described as

$$\hat{\boldsymbol{p}}_2 = Ad_{\hat{R}} \hat{\boldsymbol{p}}_1.$$

To investigate the transformation, we need to integrate the translation. This can be done in dual quaternions representation. To this end, we need to define the point in dual quaternion form, $\breve{P}_1 = \langle \hat{I}, \hat{\boldsymbol{p}}_1 \rangle$. The rotation $\hat{R}$ followed by translation $\hat{\boldsymbol{t}}$ can be lumped as transformation dual quaternion

$$\breve{T} = \left\langle \hat{R}, \frac{1}{2} \hat{\boldsymbol{t}} \circ \hat{R} \right\rangle, \tag{11}$$

and the transferred point is obtained via adjoint mapping of dual quaternions, *Definition 2.2.4*, as

$$\breve{P}_2 = Ad^2_{\breve{T}} \breve{P}_1.$$

A similar transformation can be applied to a line ℓ_1 (*cf. Definition 2.2.6*)

$$\ell_2 = Ad_{\breve{T}} \ell_1. \tag{12}$$

According to Chasles' theorem (*cf.* Murray (2017)), this transformation can be described as a screw motion. A screw is defined by its parameters of axis line ℓ, the rotation parameter around the screw axis θ and the pitch of the screw $\mu = \frac{d}{\theta}$, where d denotes the translation parameter along the axis of the screw. The former two parameters are the same in the two methods of representation. The challenge of this duo lies under extracting d from $\hat{\boldsymbol{t}}$. Exploiting Rodrigues' rotation description, Daniilidis (1999) shows

$$\hat{\boldsymbol{p}} \times \hat{\boldsymbol{l}} = \frac{1}{2} \left(\hat{\boldsymbol{t}} \times \hat{\boldsymbol{l}} + \left(\hat{\boldsymbol{t}} - d\hat{\boldsymbol{l}} \right) \cot\left(\frac{\theta}{2}\right) \right).$$

Defining dual angle $\bar{\theta} = \langle \theta, d \rangle$, it can be shown

$$\breve{S} = \left[\cos\left(\frac{\bar{\theta}}{2}\right), \sin\left(\frac{\bar{\theta}}{2}\right) \ell \right] (\equiv \breve{R}), \tag{13}$$

with $\breve{S}$ defining the screw and $\breve{R}$ from *Definition 2.2.2*. Tacking *Lemma 2.4* and *Definition 2.2.6* into account, we have

$$\begin{aligned}\breve{S} &= \exp\left(\left[\bar{0}, \frac{\bar{\theta}}{2} \diamond \ell\right]\right) \\ &= \exp\left(\frac{\theta}{2}\left[\bar{0}, \langle 1\,,\, \mu\rangle \diamond \left\langle \hat{\boldsymbol{l}}\,,\, \hat{\boldsymbol{p}} \times \hat{\boldsymbol{l}}\right\rangle\right]\right).\end{aligned} \tag{14}$$

3.2 Manipulator Kinematics

We exploit the mathematical procedure in *Sections 2* and *3.1* to formulate the kinematics of manipulators consisting of n joints. For this description, without loss of generality, we choose the base coordinate of the robot as the reference coordinate system. The axis $\hat{\boldsymbol{l}}_{ee}$ shall be chosen as the direction of the approach of the end-effector (conventionally $\hat{\boldsymbol{z}}_{ee}$). The point $\hat{\boldsymbol{p}}_{ee}$ would be selected as the position of the end-effector. For the joint screws, the action direction of joint (*i.e.* rotation axis for the revolute joints and sliding axis for prismatic joints) are chosen as $\hat{\boldsymbol{l}}_m$. The point $\hat{\boldsymbol{p}}_m$ shall be chosen as a point located on the joint. The control variable in the joint state are the dual angles of the joint screws

$$\breve{\boldsymbol{\theta}} = \left(\bar{\theta}_1, \bar{\theta}_2, \cdots, \bar{\theta}_m, \cdots, \bar{\theta}_n\right). \tag{15}$$

For revolute joints $d = 0$ and for prismatic joints $\theta = 0$.

Note the pose of end-effector of the robot by $\breve{P}_{ee}$. We define the home pose of the end-effector as $\breve{P}_{ee,home}$ with $\breve{\boldsymbol{\theta}} = \breve{\boldsymbol{\theta}}_{home}$. Besides, the screws of the joints of robot are defined as ($m \in \{1, 2, \cdots, n\}$)

$$\breve{J}_m = \left[\cos(\frac{\bar{\theta}_m}{2}), \sin(\frac{\bar{\theta}_m}{2}) \diamond Ad_{\{\breve{J}_{m-1}\}}\ell_{m,home}\right], \tag{16}$$

where

$$\{\breve{J}_k\} = \prod_{i=k}^{1} \breve{J}_i = \breve{J}_k \diamond \breve{J}_{k-1} \diamond \cdots \diamond \breve{J}_1. \tag{17}$$

Thus

$$\breve{P}_{ee} = Ad_{\{\breve{J}_n\}}\breve{P}_{ee,home}. \tag{18}$$

Of course this manner of representation, which is singularity free (*cf.* Funda and Paul (1990); Funda et al. (1990)), can be generalized to any other joint $\breve{J}_m$ of the robot.

4. CONTROLLER

Given new set points for the end-effector of the robot from the motion planner ($\breve{P}_{ee}$, see Fig. 1) the pose error should be determined. Using the mathematical properties of the dual quaternions, we define the pose error in global coordinate system via

$$\breve{E}_{rr} = \breve{P}_{set} \diamond \breve{P}^*_{ee}, \tag{19}$$

with $\breve{E}_{rr}$ and $\breve{P}_{set}$ denoting the pose error and set pose respectively.

4.1 Control Law

Considering the twist dual vector $\breve{\Xi} = \left\langle \hat{\boldsymbol{\omega}}\,,\, \dot{\hat{\boldsymbol{d}}} + \hat{\boldsymbol{p}} \times \hat{\boldsymbol{\omega}}\right\rangle$, we define the *special proportional-derivative* $\breve{\Xi}$ kinematics control law as

$$\breve{\Xi} = -2\breve{K} \odot \left(\ln^{\mathcal{DH}}\left(\breve{E}_{rr}\right) - \breve{K}^D \odot \nabla_{\{\theta,d\}} \ln^{\mathcal{DH}}\left(\breve{E}_{rr}\right)\right), \tag{20}$$

where $\breve{K} = \left\langle \hat{\boldsymbol{k}}_o\,,\, \hat{\boldsymbol{k}}_p\right\rangle$ and $\breve{K}^D = \left\langle \hat{\boldsymbol{k}}^D_o\,,\, \hat{\boldsymbol{k}}^D_p\right\rangle$ represent dual vectors of positive real constants and $\odot$ denotes Hadamard product operator. A schematic of the control loop is presented in Fig. 1. In the following we consider the controller in two formats: Ξ_1 with $\breve{K}^D = \breve{0}$ and Ξ_2 with $\breve{K}^D > \breve{0}$. The advantage of the $\breve{\Xi}_2$ over $\breve{\Xi}_1$ is the sensitivity to the error evolution that results in higher speed of convergence, thus less CPU effort (see *Section 5.1*). To apply the controller, we use (7) and (14) to simplify the $\ln^{\mathcal{DH}}(\breve{P})$ as

$$\begin{aligned}\ln^{\mathcal{DH}}\left(\breve{P}\right) &= \left[\bar{0}, \frac{\bar{\theta}}{2} \diamond \ell\right] \\ &= \frac{1}{2}\left\langle \theta\hat{\boldsymbol{l}}\,,\, \theta\left(\hat{\boldsymbol{p}} \times \hat{\boldsymbol{l}}\right) + d\hat{\boldsymbol{l}}\right\rangle \\ &= \frac{1}{2}\left\langle \theta\hat{\boldsymbol{l}}\,,\, \theta\hat{\boldsymbol{m}} + d\hat{\boldsymbol{l}}\right\rangle \\ &= \frac{1}{2}\left\langle \hat{\boldsymbol{\theta}}_l\,,\, \hat{\boldsymbol{\theta}}_m + \hat{\boldsymbol{d}}_l\right\rangle.\end{aligned} \tag{21}$$

4.2 Stability Analysis of the Controller

Equation (9) (which clearly is positive definite) would be chosen as Lyapunov function candidate V to investigate the stability of the controller, *i.e.*

$$\mathsf{V} = \left\|\ln^{\mathcal{DH}}\left(\breve{E}_{rr}\right)\right\| = \alpha\left|\hat{\boldsymbol{\theta}}_{l,err}\right| + \beta\left|\hat{\boldsymbol{\theta}}_{m,err} + \hat{\boldsymbol{d}}_{l,err}\right| \tag{22}$$

$$= \left\|\ln^{\mathcal{DH}}\left(\breve{E}_{rr}\right)\right\| = \alpha\left|\hat{\boldsymbol{\theta}}_{l,err}\right| + \beta\left|\hat{\boldsymbol{t}}'_{err}\right|. \tag{23}$$

Note that $\hat{\boldsymbol{t}}'_{err} = \hat{\boldsymbol{\theta}}_{m,err} + \hat{\boldsymbol{d}}_{l,err}$ is parallel to translation vector $\hat{\boldsymbol{t}}_{err}$ (*cf. Section 3.1*). Hence, we can safely replace it in (23) with $\hat{\boldsymbol{t}}_{err}$, substituting β with $\gamma \in \mathcal{R}_+$ (for the sake of simplicity of notation we drop the subscript *err* hereafter)

$$\mathsf{V} = \left\|\ln^{\mathcal{DH}}\left(\breve{E}_{rr}\right)\right\| = \alpha\left|\hat{\boldsymbol{\theta}}_l\right| + \gamma\left|\hat{\boldsymbol{t}}\right|. \tag{24}$$

Differentiating (23) yields

$$\dot{\mathsf{V}} = \alpha\hat{\boldsymbol{\theta}}_l \cdot \dot{\hat{\boldsymbol{\theta}}}_l + \gamma\hat{\boldsymbol{t}} \cdot \dot{\hat{\boldsymbol{t}}}. \tag{25}$$

To investigate the stability of $\breve{\Xi}$, we expand the gradient part of (20) using exponential form of $\breve{E}_{rr}$ (*cf. Lemma 2.4*) and considering the fact that the inverse of a unit dual quaternion is its conjugate (*cf.* Kavan et al. (2008))

$$\nabla_{\{\theta,d\}} \ln^{\mathcal{DH}}\left(\breve{E}_{rr}\right) = \left(\frac{\partial \exp\left(\left[\bar{0}\,,\, \frac{\bar{\theta}}{2} \diamond \ell\right]\right)}{\partial\theta} + \frac{\partial \exp\left(\left[\bar{0}\,,\, \frac{\bar{\theta}}{2} \diamond \ell\right]\right)}{\partial d}\right) \diamond \breve{E}^*_{rr}. \tag{26}$$

Using the derivation rule of exponential functions and chain rule, we have

$$\begin{aligned}\nabla_{\{\theta,d\}} \ln^{\mathcal{DH}}\left(\breve{E}_{rr}\right) &= \left(\frac{\partial\left(\left[\bar{0}\,,\, \frac{\bar{\theta}}{2} \diamond \ell\right]\right)}{\partial\theta} + \frac{\partial\left(\left[\bar{0}\,,\, \frac{\bar{\theta}}{2} \diamond \ell\right]\right)}{\partial d}\right) \diamond \underbrace{\breve{E}_{rr} \diamond \breve{E}^*_{rr}}_{\breve{I}} \\ &= \frac{1}{2}\left(\langle 1, 0\rangle \diamond \left\langle \hat{\boldsymbol{l}}, \hat{\boldsymbol{p}} \times \hat{\boldsymbol{l}}\right\rangle + \langle 0, 1\rangle \diamond \left\langle \hat{\boldsymbol{l}}, \hat{\boldsymbol{p}} \times \hat{\boldsymbol{l}}\right\rangle\right) \diamond \breve{I} \\ &= \frac{1}{2}\left\langle \hat{\boldsymbol{l}}, \hat{\boldsymbol{p}} \times \hat{\boldsymbol{l}} + \hat{\boldsymbol{l}}\right\rangle.\end{aligned} \tag{27}$$

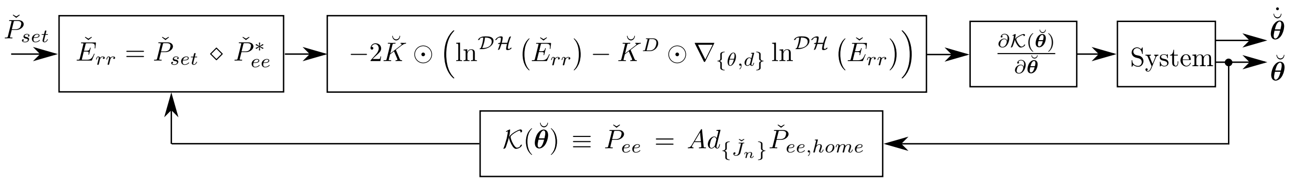

Fig. 1. Schematic of the motion control loop, as described in *Section 4*

Therefore $\breve{\Xi}$ can be written as

$$\begin{aligned}\breve{\Xi} &= -2\breve{K} \odot \left(\ln^{\mathcal{DH}}\left(\breve{E}_{rr}\right) + \breve{K}^D \odot \frac{1}{2}\left\langle \hat{\boldsymbol{l}}, \hat{\boldsymbol{p}} \times \hat{\boldsymbol{l}} + \hat{\boldsymbol{l}} \right\rangle\right) \\ &= -\breve{K} \odot \left(\left\langle \hat{\boldsymbol{\theta}}_l \,, \hat{\boldsymbol{\theta}}_m + \hat{\boldsymbol{d}}_l \right\rangle + \breve{K}^D \odot \left\langle \hat{\boldsymbol{l}}, \hat{\boldsymbol{p}} \times \hat{\boldsymbol{l}} + \hat{\boldsymbol{l}} \right\rangle\right). \end{aligned} \tag{28}$$

From (20) and (28) we have

$$\hat{\boldsymbol{\omega}} = \dot{\hat{\boldsymbol{\theta}}}_l = -\hat{\boldsymbol{k}}_o \odot \hat{\boldsymbol{\theta}}_l - \hat{\boldsymbol{k}}_o \odot \hat{\boldsymbol{k}}^D_o \odot \hat{\boldsymbol{l}}, \tag{29}$$

$$\dot{\hat{\boldsymbol{t}}} = -\hat{\boldsymbol{k}}_p \odot \hat{\boldsymbol{t}}' - \hat{\boldsymbol{k}}_p \odot \hat{\boldsymbol{k}}^D_p \odot \left(\hat{\boldsymbol{m}} + \hat{\boldsymbol{l}}\right). \tag{30}$$

Substituting (29) and (30) in (25), we have

$$\begin{aligned}\dot{\mathsf{V}} &= \alpha\hat{\boldsymbol{\theta}}_l \cdot \left(-\hat{\boldsymbol{k}}_o \odot \hat{\boldsymbol{\theta}}_l\right) + \alpha\theta\hat{\boldsymbol{l}} \cdot \left(-\hat{\boldsymbol{k}}_o \odot \hat{\boldsymbol{k}}^D_o \odot \hat{\boldsymbol{l}}_l\right) \\ &+ \gamma\hat{\boldsymbol{t}} \cdot \left(-\hat{\boldsymbol{k}}_p \odot \hat{\boldsymbol{t}}'\right) + \gamma\hat{\boldsymbol{t}} \cdot \left(-\hat{\boldsymbol{k}}_p \odot \hat{\boldsymbol{k}}^D_p \odot \left(\hat{\boldsymbol{m}} + \hat{\boldsymbol{l}}\right)\right), \end{aligned} \tag{31}$$

which proves $\dot{\mathsf{V}}$ is negative definite. Besides, $\dot{\mathsf{V}} \leq -k^*\mathsf{V}$, with k^* denoting the smallest constant in $\hat{\boldsymbol{k}}_o$ and $\hat{\boldsymbol{k}}_p$, which guarantees $\breve{\Xi}$ is globally exponentially stable.

5. DISCUSSION

The motion planning algorithm delivers the desired poses of end-effector $\breve{P}_{ee}$, based on the dynamic and the shape of the environment. In case of wide-distance set points, interpolation techniques (such as spherical interpolation for position (see *e.g.* Buss and Fillmore (2001)) or SLERP for orientation (see *e.g.* Shoemake (1985))) shall be applied to guarantee a smooth motion control. To do so, we need to extract the amount of angle of rotation θ_{err} and the vector $\hat{\boldsymbol{l}}_{err}$, about which the rotation should take place, from $\breve{E}_{rr}$

$$\hat{P}_{err} = \breve{e}_{rr}, \tag{32}$$

$$\theta_{err} = 2\cos^{-1}\left(\hat{p}_{err}\right), \tag{33}$$

$$\hat{\boldsymbol{l}}_{err} = \left(\sin\left(\frac{\theta_{err}}{2}\right)\right)^{-1} \hat{\boldsymbol{p}}_{err}. \tag{34}$$

Then the interpolation can simply be carried out on the angle element θ_{err}. The interpolated angle representations of rotation along the path are the adjoints of $\breve{P}_{ee}$ along the interpolated quaternions.

5.1 Implementation - Computational Cost

To examine the introduced controllers a 2-path task has been modelled. Two serial manipulators Universal Robots UR5 and KUKA Agilus KR6 are chosen to validate the results of the proposed controllers. We consider $\breve{\boldsymbol{\theta}}_{home-UR5} = \left(-\frac{\pi}{4}, -\frac{\pi}{4}, -\frac{\pi}{2}, -\frac{3\pi}{4}, \frac{\pi}{4}, \frac{\pi}{4}\right)$ for Universal Robots UR5 and $\breve{\boldsymbol{\theta}}_{home-KR6} = \left(0, -\frac{\pi}{2}, \frac{\pi}{2}, 0, \frac{\pi}{2}, 0\right)$ for KUKA Agilus KR6. The robots in their home position (in bold) and the 2-path task are shown in Fig. 2 (Note: $\hat{\boldsymbol{l}}_{ee}$ is shown in blue and $\hat{\boldsymbol{m}}_{ee}$ is shown in red).

Table 1. Total CPU Time [μs]

	$\breve{\Xi}_1$		$\breve{\Xi}_2$	
	Path 1	Path 2	Path 1	Path 2
UR5	1161284	1123023	882962	842149
KR6	1189224	1118307	893816	842153

The two controllers are implemented to control the kinematic of robots and generate the motion in joint space $\breve{\boldsymbol{\theta}}$. Application oriented time functions and trajectory planning methods can be applied to the generated motion in joint space to compute the trajectory for the manipulators. The evolution of the pose errors are shown in Fig. 4. The errors are split into translation errors $\hat{\boldsymbol{t}}_{err}$ and rotation errors $\hat{\boldsymbol{\theta}}_{err} = \theta_{err}\hat{\boldsymbol{l}}_{err}$ (*cf.* (1) and (11)). The horizontal axis of the plots represent the amount of the iteration over the control loops. The picks on the error diagram happen on introduction of the new set point from the motion planner to the motion controller.
The computational efficiency of dual quaternions is proven through numerous studies (see for instance Funda and Paul (1990); Wang and Zhu (2014)). There has been different reports about the amount of computational effort of different representation attitudes (homogenous transformation matrices, unit dual quaternions, transformation angle axis, etc.) though. Differences arise mainly from the implementation of the algorithm. Here we discuss the efficiency of the $\breve{\Xi}_1$ and $\breve{\Xi}_2$. The computational effort for the later is obviously more than the former, but the convergence rate of $\breve{\Xi}_2$ is higher than $\breve{\Xi}_1$. The total CPU (Intel® Core™ i7-4600M 2.90GHz×4) time to compute the complete motion in joint space as well as the mean CPU time for each of the via points in microseconds are reported in Table 1 and Fig. 3 respectively.

6. CONCLUSION

The main result of this paper is the presentation of kinematic control of serial manipulators using Clifford algebra of unit dual quaternions operations and introduction of the new control scheme *special proportional-derivative* $\breve{\Xi}$. The necessary mathematical background to model the serial manipulators using dual quaternions and screw theory are presented.

The stability of the controller is proven by means of a proper Lyapunov function candidate. The performance of the controller is examined via an exemplary 2-path motion. The CPU effort over these implementations are presented.

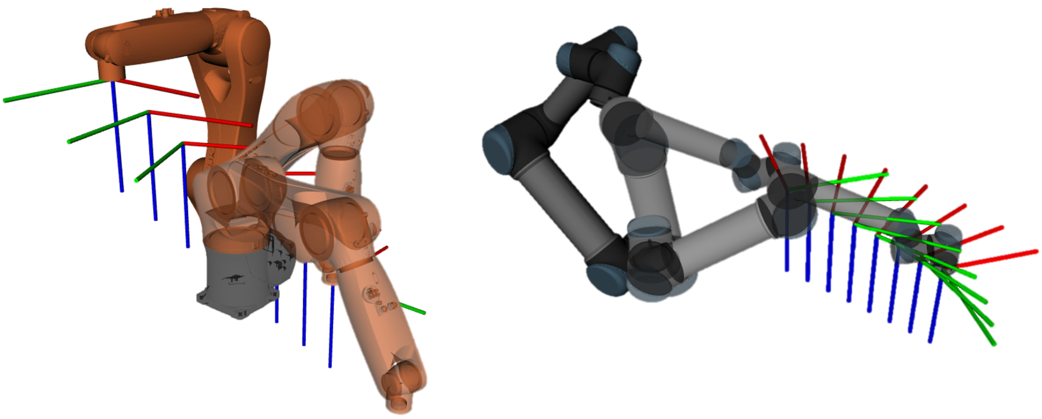

Fig. 2. The home position of the manipulators (in bold) and the middle and end positions (transparent) Left; KUKA Agilus KR6 and path 1, Right; Universal Robots UR5 and path 2

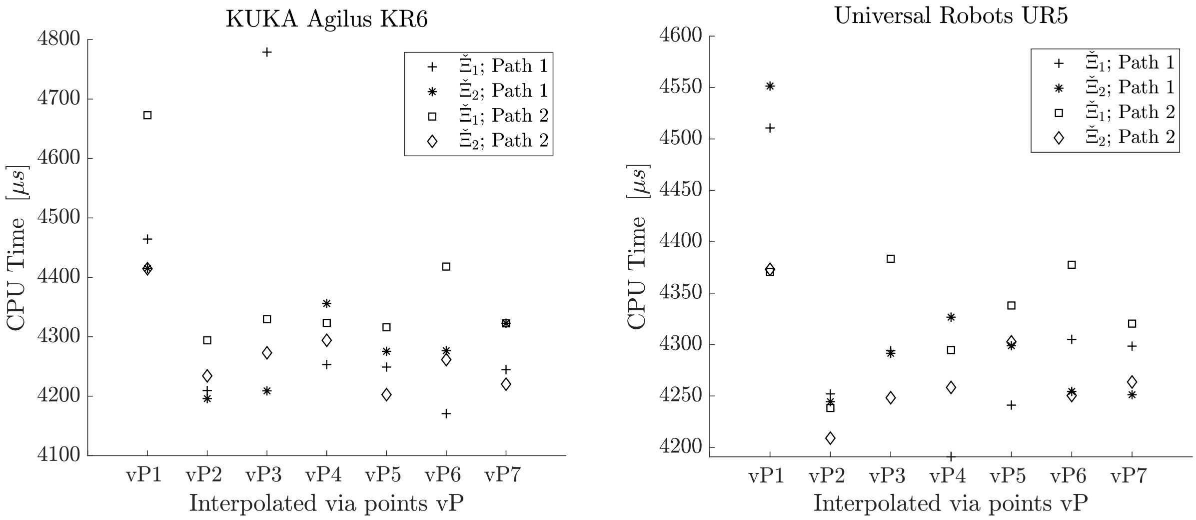

Fig. 3. The average CPU time over iterations to compute the joint space motion at each via point - see Fig. 4 for amount of iterations and evolution of error

REFERENCES

Buss, S.R. and Fillmore, J.P. (2001). Spherical averages and applications to spherical splines and interpolation. *ACM Transactions on Graphics (TOG)*, 20(2), 95–126.

Clifford, W.K. (1873). Preliminary sketch of biquaternions. In *Proceedings of the London Mathematical Society*, 381–395.

Daniilidis, K. (1999). Hand-eye calibration using dual quaternions. *The International Journal of Robotics Research*, 18(3), 286–298.

Dapeng, H., Qing, W., and Li Zexiang (2007). Attitude control based on the lie-group structure of unit quaternions. In *2007 Chinese Control Conference*, 326–331. doi:10.1109/CHICC.2006.4347101.

Diebel, J. (2006). Representing attitude: Euler angles, unit quaternions, and rotation vectors. *Matrix*, 58(15-16), 1–35.

Funda, J. and Paul, R.P. (1990). A computational analysis of screw transformations in robotics. *IEEE Transactions on Robotics and Automation*, 6(3), 348–356.

Funda, J., Taylor, R.H., and Paul, R.P. (1990). On homogeneous transforms, quaternions, and computational efficiency. *IEEE Transactions on Robotics and Automation*, 6(3), 382–388.

Hamilton, W.R. (1848). Xi. on quaternions; or on a new system of imaginaries in algebra. *The London, Edinburgh, and Dublin Philosophical Magazine and Journal of Science*, 33(219), 58–60.

Han, D., Wei, Q., Li, Z., and Sun, W. (2008). Control of oriented mechanical systems: A method based on dual quaternion. volume 41, 3836–3841. Elsevier.

Hestenes, D. and Sobczyk, G. (2012). *Clifford algebra to geometric calculus: a unified language for mathematics and physics*, volume 5. Springer Science & Business Media.

Kavan, L., Collins, S., Žára, J., and O'Sullivan, C. (2008). Geometric skinning with approximate dual quaternion blending. *ACM Transactions on Graphics (TOG)*, 27(4), 105.

Kim, M.J., Kim, M.S., and Shin, S.Y. (1996). A compact differential formula for the first derivative of a unit quaternion curve. *The Journal of Visualization and Computer Animation*, 7(1), 43–57.

Marsden, J.E. and Ratiu, T.S. (2013). *Introduction to mechanics and symmetry: a basic exposition of classical mechanical systems*, volume 17. Springer Science &

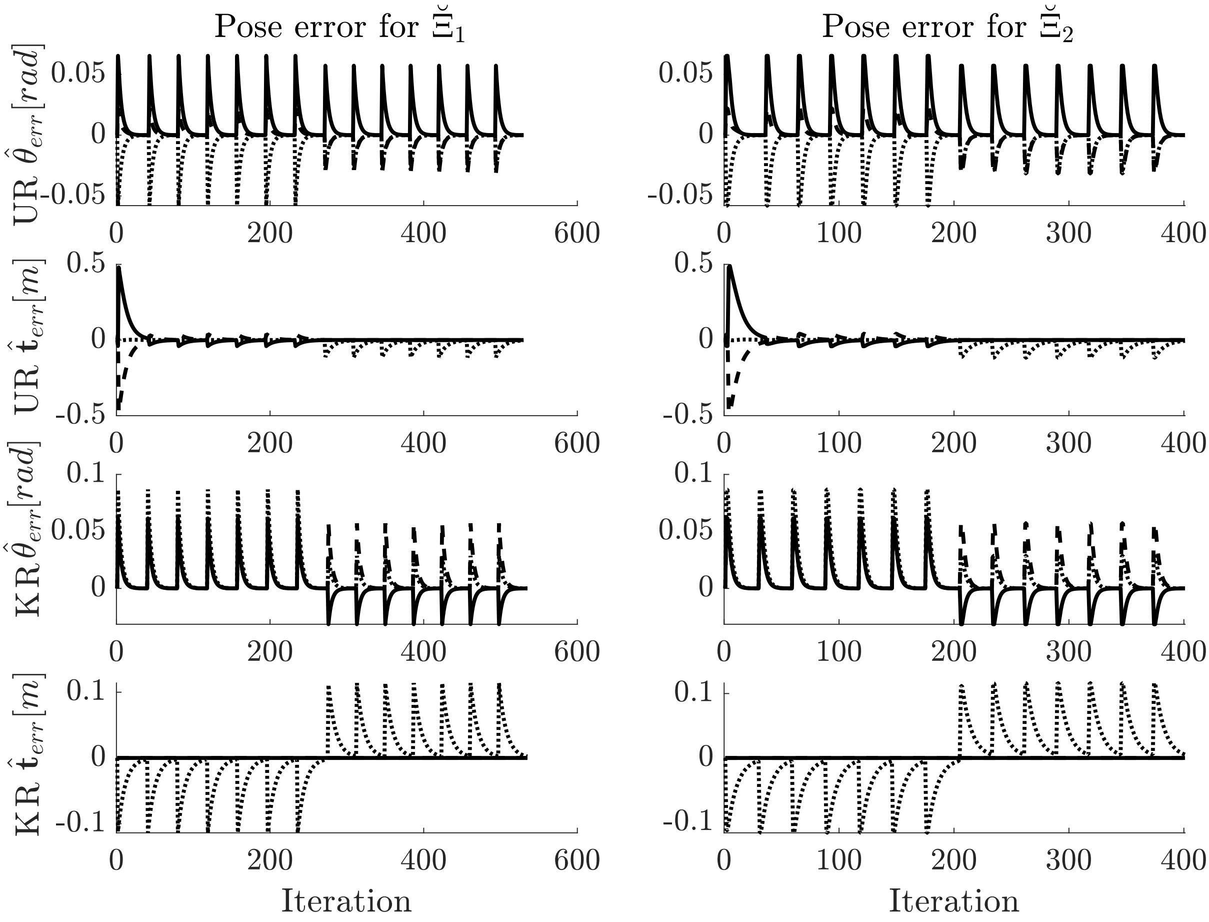

Fig. 4. Comparison of the evolution of the pose error of implementation of the two control laws $\check{\Xi}_1$ and $\check{\Xi}_2$

Business Media.

Murray, R.M. (2017). *A mathematical introduction to robotic manipulation.* CRC press.

Olsson, T., Bengtsson, J., Robertsson, A., and Johansson, R. (2003). Visual position tracking using dual quaternions with hand-eye motion constraints. In *2003 IEEE International Conference on Robotics and Automation (Cat. No. 03CH37422)*, volume 3, 3491–3496. IEEE.

Özgür, E. and Mezouar, Y. (2016). Kinematic modeling and control of a robot arm using unit dual quaternions. *Robotics and Autonomous Systems*, 77, 66–73. doi: 10.1016/j.robot.2015.12.005.

Perez-Gracia, A. and McCarthy, J.M. (2006). Kinematic synthesis of spatial serial chains using clifford algebra exponentials. *Proceedings of the Institution of Mechanical Engineers, Part C: Journal of Mechanical Engineering Science*, 220(7), 953–968.

Shoemake, K. (1985). Animating rotation with quaternion curves. In *ACM SIGGRAPH computer graphics*, volume 19, 245–254. ACM.

Stolt, A., Linderoth, M., Robertsson, A., and Johansson, R. (2012). Robotic assembly using a singularity-free orientation representation based on quaternions. *IFAC Proceedings Volumes*, 45(22), 549–554.

Wang, X., Han, D., Yu, C., and Zheng, Z. (2012). The geometric structure of unit dual quaternion with application in kinematic control. *Journal of Mathematical Analysis and Applications*, 389(2), 1352–1364.

Wang, X. and Zhu, H. (2014). On the comparisons of unit dual quaternion and homogeneous transformation matrix. *Advances in Applied Clifford Algebras*, 24(1), 213–229. doi:10.1007/s00006-013-0436-y. URL `https://doi.org/10.1007/s00006-013-0436-y`.

Appendix A. QUATERNIONS

Quaternions $\hat{Q}$, four dimensional pseudo vectors over the elements of an algebraic field like real numbers set $\mathbb{H} \simeq \mathbb{R}^4$, consist of real $\hat{q}$ and lateral (pure quaternion) $\hat{\boldsymbol{q}}$ parts

$$\hat{Q} = [\hat{q}, \hat{\boldsymbol{q}}] \,. \tag{A.1}$$

Addition over the set of quaternions is carried out component wise,

$$\hat{Q}_1 + \hat{Q}_2 = [\hat{q}_1 + \hat{q}_2, \hat{\boldsymbol{q}}_1 + \hat{\boldsymbol{q}}_2]. \tag{A.2}$$

Multiplication in quaternions, denoted by $\circ$, is defined by

$$\hat{Q}_1 \circ \hat{Q}_2 = [\hat{q}_1\, \hat{q}_2 - \hat{\boldsymbol{q}}_1 \cdot \hat{\boldsymbol{q}}_2, \hat{q}_1\, \hat{\boldsymbol{q}}_2 + \hat{q}_2\, \hat{\boldsymbol{q}}_1 + \hat{\boldsymbol{q}}_1 \times \hat{\boldsymbol{q}}_2]. \tag{A.3}$$

The conjugate, the norm and the inverse of quaternions are defined as

$$\hat{Q}^* = [\hat{q}, -\hat{\boldsymbol{q}}], \tag{A.4}$$

$$\left|\hat{Q}\right| = \sqrt{\hat{Q} \circ \hat{Q}^*}, \tag{A.5}$$

$$\hat{Q}^{-1} = \left|\hat{Q}\right|^{-2} \hat{Q}^*. \tag{A.6}$$

Note that

$$\left(\hat{Q}_1 \circ \hat{Q}_2\right)^* = \hat{Q}_2^* \circ \hat{Q}_1^*. \quad (A.7)$$

We can obtain the dot and cross multiplications of pure quaternions as

$$\begin{aligned} \hat{\boldsymbol{q}}_1 \cdot \hat{\boldsymbol{q}}_2 &= -\frac{1}{2}\left(\hat{\boldsymbol{q}}_1 \circ \hat{\boldsymbol{q}}_2 + \hat{\boldsymbol{q}}_2 \circ \hat{\boldsymbol{q}}_1\right), \\ \hat{\boldsymbol{q}}_1 \times \hat{\boldsymbol{q}}_2 &= \frac{1}{2}\left(\hat{\boldsymbol{q}}_1 \circ \hat{\boldsymbol{q}}_2 - \hat{\boldsymbol{q}}_2 \circ \hat{\boldsymbol{q}}_1\right). \end{aligned} \quad (A.8)$$

Appendix B. DUAL QUATERNIONS

B.1 Dual Numbers

Dual numbers $\bar{d}$ are two dimensional numbers over the elements of an algebraic field like real numbers set

$$\bar{d} = \bar{d}_p + \epsilon \bar{d}_d = \langle \bar{d}_p\,,\, \bar{d}_d \rangle \in \mathbb{D} \backsimeq \mathbb{R}^2, \quad (B.1)$$

with ϵ as nilpotent Clifford unit that squares to 0 and subscripts p and d denoting primal and dual parts respectively. The addition and multiplication, denoted by $\diamond$, of dual numbers are defined as

$$\bar{d}_1 + \bar{d}_2 = \langle \bar{d}_{p,1} + \bar{d}_{p,2}\,,\, \bar{d}_{d,1} + \bar{d}_{d,2} \rangle, \quad (B.2)$$

$$\bar{d}_1 \diamond \bar{d}_2 = \langle \bar{d}_{p,1}\,\bar{d}_{p,2}\,,\, \bar{d}_{p,1}\,\bar{d}_{d,2} + \bar{d}_{p,2}\,\bar{d}_{d,1} \rangle. \quad (B.3)$$

The conjugate and the inverse in dual numbers are defined as

$$\bar{d}^* = \langle \bar{d}_p\,,\, -\bar{d}_d \rangle, \quad (B.4)$$

$$\bar{d}^{-1} = \langle \bar{d}_p^{-1}\,,\, -\bar{d}_p^{-1}\,\bar{d}_d \rangle. \quad (B.5)$$

B.2 Dual Quaternions

Dual quaternions $\breve{D}$ are the duals over the elements of quaternion field $\mathbb{H}$, thus $\breve{D} \in \mathbb{DH} \backsimeq \mathbb{H}^2$:

$$\breve{Q} = \left\langle \breve{d}\,,\, \breve{\boldsymbol{d}} \right\rangle,\ \breve{d}\,\&\,\breve{\boldsymbol{d}} \in \mathbb{H}. \quad (B.6)$$

Therefore, combining the mathematical arithmetic of quaternions and those of dual numbers, one can explore the operations on the set of dual quaternions. For dual quaternions 3 different conjugates shall be defined

$$\breve{D}^{*_0} = \left\langle \breve{d}\,,\, -\breve{\boldsymbol{d}} \right\rangle, \quad (B.7)$$

$$\breve{D}^* = \breve{D}^{*_1} = \left\langle \breve{d}^*\,,\, \breve{\boldsymbol{d}}^* \right\rangle = \left[\breve{d}\,,\, -\breve{\boldsymbol{d}}\right] \quad (B.8)$$

$$\breve{D}^{*_2} = \left\langle \breve{d}^*\,,\, -\breve{\boldsymbol{d}}^* \right\rangle. \quad (B.9)$$

If not noted explicitly, the $\breve{D}^*$ is considered as the standard form of the conjugation of dual quaternions. We have

$$\left(\breve{D}_1 \diamond \breve{D}_2\right)^* = \breve{D}_2^* \diamond \breve{D}_1^*. \quad (B.10)$$

The norm of dual quaternions are defined as

$$\left|\breve{D}\right| = \sqrt{\breve{D} \diamond \breve{D}^*}. \quad (B.11)$$

The dot and cross multiplication for the dual quaternions composed of pure quaternions, also known as dual vectors, are defined as

$$\begin{aligned} \breve{D}_1 \cdot \breve{D}_2 &= \left\langle \breve{d}_1 \cdot \breve{d}_2\,,\, \breve{d}_1 \cdot \breve{\boldsymbol{d}}_2 + \breve{d}_2 \cdot \breve{\boldsymbol{d}}_1 \right\rangle, \\ \breve{D}_1 \times \breve{D}_2 &= \left\langle \breve{d}_1 \times \breve{d}_2\,,\, \breve{d}_1 \times \breve{\boldsymbol{d}}_2 + \breve{d}_2 \times \breve{\boldsymbol{d}}_1 \right\rangle. \end{aligned} \quad (B.12)$$

Appendix C. PROOF OF *LEMMA 2.4*

We expand the exponential form of $\breve{D} = \exp\left(\left[\bar{0}, \frac{\bar{\theta}}{2} \diamond \ell\right]\right)$ via Taylor series

$$\begin{aligned} \breve{D} = \exp\left(\left[\bar{0}, \frac{\bar{\theta}}{2} \diamond \ell\right]\right) &= 1 + \left[\bar{0}, \frac{\bar{\theta}}{2} \diamond \ell\right] \\ &+ \frac{1}{2!}\left(\left(\left[\bar{0}, \frac{\bar{\theta}}{2} \diamond \ell\right]\right) \diamond \left(\left[\bar{0}, \frac{\bar{\theta}}{2} \diamond \ell\right]\right)\right) \\ + \frac{1}{3!}\left(\left(\left[\bar{0}, \frac{\bar{\theta}}{2} \diamond \ell\right]\right) \diamond \left(\left[\bar{0}, \frac{\bar{\theta}}{2} \diamond \ell\right]\right) \diamond \left(\left[\bar{0}, \frac{\bar{\theta}}{2} \diamond \ell\right]\right)\right) \\ &+ \cdots. \end{aligned} \quad (C.1)$$

Knowing $\bar{\theta} = \langle \theta\,,\, d \rangle$ and $\ell = \left\langle \hat{\boldsymbol{l}}\,,\, \hat{\boldsymbol{p}} \times \hat{\boldsymbol{l}} \right\rangle$ we have

$$\frac{\bar{\theta}}{2} \diamond \ell = \frac{\theta}{2}\,\langle 1\,,\, \mu \rangle \diamond \left\langle \hat{\boldsymbol{l}}\,,\, \hat{\boldsymbol{p}} \times \hat{\boldsymbol{l}} \right\rangle = \frac{\theta}{2}\,\underbrace{\left\langle \hat{\boldsymbol{l}}\,,\, \hat{\boldsymbol{p}} \times \hat{\boldsymbol{l}} + \mu\,\hat{\boldsymbol{l}} \right\rangle}_{\breve{\boldsymbol{Z}}}. \quad (C.2)$$

with $\mu = \frac{d}{\theta}$ denoting the pitch of screw. Denote $\breve{Z} = [\bar{0}, \breve{\boldsymbol{Z}}]$. We have

$$\breve{Z} \diamond \breve{Z} = \left[-\breve{\boldsymbol{Z}} \cdot \breve{\boldsymbol{Z}}\,,\, \breve{\boldsymbol{Z}} \times \breve{\boldsymbol{Z}}\right].$$

Using the rules in *Appendices A* and *B* we obtain

$$\begin{aligned} \breve{Z}_1 &= \breve{Z} \diamond \breve{Z} &&= \left[\langle -1\,,\, -2\,\mu \rangle\,,\, \bar{\boldsymbol{0}}\right], \\ \breve{Z}_2 &= \breve{Z}_1 \diamond \breve{Z} &&= [\bar{0}, \langle -1\,,\, -3\,\mu \rangle \diamond \ell], \\ \breve{Z}_3 &= \breve{Z}_2 \diamond \breve{Z} &&= \left[\langle 1\,,\, 4\,\mu \rangle\,,\, \bar{\boldsymbol{0}}\right], \\ \breve{Z}_4 &= \breve{Z}_3 \diamond \breve{Z} &&= [\bar{0}, \langle 1\,,\, 5\,\mu \rangle \diamond \ell], \end{aligned} \quad (C.3)$$

and so on. The Taylor's series expansion of the functions $\sin(\theta)$ and $\cos(\theta)$ are known as

$$\begin{aligned} \cos(\theta) &= 1 - \frac{1}{2!}\,(\theta)^2 + \frac{1}{4!}\,(\theta)^4 - \cdots, \\ \sin(\theta) &= \theta - \frac{1}{3!}\,(\theta)^3 + \frac{1}{5!}\,(\theta)^5 - \cdots. \end{aligned} \quad (C.4)$$

Substituting (C.2) and (C.3) into (C.1), after factorization and using (C.4) we obtain

$$\begin{aligned} \breve{D} &= \exp\left(\left[\bar{0}, \frac{\bar{\theta}}{2} \diamond \ell\right]\right) \\ &= \cos\left(\frac{\theta}{2}\right) + \sin\left(\frac{\theta}{2}\right)\,\ell \\ &- \frac{\epsilon\,\mu\,\theta}{2}\,\sin\left(\frac{\theta}{2}\right) + \frac{\epsilon\,\mu\,\theta}{2}\,\cos\left(\frac{\theta}{2}\right)\,\ell, \end{aligned} \quad (C.5)$$

$$\begin{aligned} \breve{D} &= \exp\left(\left[\bar{0}, \frac{\bar{\theta}}{2} \diamond \ell\right]\right) \\ &= \left[\left\langle \cos\left(\frac{\theta}{2}\right)\,,\, -\frac{\mu\,\theta}{2}\,\sin\left(\frac{\theta}{2}\right) \right\rangle\right. \\ &\left.,\, \sin\left(\frac{\theta}{2}\right)\,\ell + \frac{\epsilon\,\mu\,\theta}{2}\,\cos\left(\frac{\theta}{2}\right)\,\ell\right]. \end{aligned} \quad (C.6)$$

After algebraic simplification we obtain

$$\breve{D} = \exp\left(\left[\bar{0}, \frac{\bar{\theta}}{2} \diamond \ell\right]\right) = \left[\cos\left(\frac{\bar{\theta}}{2}\right)\,,\, \sin\left(\frac{\bar{\theta}}{2}\right)\,\ell\right]. \quad (C.7)$$

For similar proofs see Kim et al. (1996); Wang et al. (2012).